



## Research Paper

# Magnetic ordering in Co<sup>2+</sup>-containing layered double hydroxides via the low-temperature heat capacity and magnetisation study

Yu.G. Pashkevich<sup>a</sup>, E.L. Fertman<sup>b</sup>, A.V. Fedorchenko<sup>b</sup>, D.E.L. Vieira<sup>c</sup>, C.S. Neves<sup>c</sup>,  
R.Yu. Babkin<sup>a</sup>, A.A. Lyogenkaya<sup>b</sup>, R. Tarasenko<sup>d</sup>, V. Tkáč<sup>d</sup>, E. Čižmár<sup>d</sup>, A. Feher<sup>d</sup>,  
A.N. Salak<sup>c,\*</sup>

<sup>a</sup> O. Galkin Donetsk Institute for Physics and Engineering of NASU, 03028 Kyiv, Ukraine

<sup>b</sup> B. Verkin Institute for Low Temperature Physics and Engineering of NASU, 61103 Kharkiv, Ukraine

<sup>c</sup> Department of Materials and Ceramic Engineering, CICECO – Aveiro Institute of Materials, University of Aveiro, 3810-193 Aveiro, Portugal

<sup>d</sup> Institute of Physics, Faculty of Science, P.J. Šafárik University in Košice, 04154 Košice, Slovakia



## ARTICLE INFO

## Keywords:

Layered double hydroxide  
Heat capacity  
Schottky-like anomaly  
Magnetic ordering

## ABSTRACT

The low-temperature heat capacity and the magnetisation of Co<sub>n</sub><sup>2+</sup>Al<sup>3+</sup> layered double hydroxides (LDH) with the cobalt-to-aluminium ratio  $n = 2$  and 3 and intercalated with different anions have been studied in a wide range of magnetic fields up to 50 kOe. The heat capacity,  $C(T)$ , was found to demonstrate a Schottky-like anomaly observed as a broad local maximum in the temperature dependence below 10 K. The effect is caused by a splitting of the ground-state Kramers doublet of Co<sup>2+</sup> in the internal exchange field and correlates with magnetic ordering in these LDH. In low applied fields, the temperature-dependent  $dc$  magnetic susceptibility demonstrates a pronounced rise, which is associated with an onset of magnetic ordering. Both the heat capacity anomaly and the magnetic susceptibility peak are more pronounced for the LDH with  $n = 2$  than for those with  $n = 3$ . This feature is associated with an excess of the honeycomb-like Co–Al coordination (which corresponds to a 2:1 Co–Al ordering) over the statistical cation distribution in Co<sub>2</sub>Al LDH, while a rather random cobalt-aluminium distribution is typical for Co<sub>3</sub>Al LDH. The temperature of the Schottky-like anomaly measured in a zero field is independent of the interlayer distance. Application of the magnetic field results in a widening of the anomaly range and a shift to higher temperatures. The observed experimental data are typical for a cluster spin glass ground state.

## 1. Introduction

Layered double hydroxides (LDH) are lamellar inorganic solids, also known as hydrotalcites and anionic clays [Rives, 2001; Duan and Evans, 2006]. Most LDH are mixed divalent-trivalent metal hydroxides that form positively charged ( $M^{2+}, M^{3+}$ )OH<sub>2</sub> layers with anions and water molecules intercalated in between. LDH crystallize in hexagonal symmetry with the  $c$ -axis perpendicular to the hydroxide layers. Six hydroxyl ions surround each metal cation in the hydroxide layers forming edge-shared MO<sub>6</sub> octahedra in which the O–H bonds are perpendicular to the plane of the layers. The chemical composition of an LDH can be represented by the general formula  $M_{1-x}^{2+}M_x^{3+}(\text{OH})_2(A^y)_{x/y} \cdot z\text{H}_2\text{O}$ , where  $A^y$  is an anion or a combination of different ionic species compensating the positive charge of the hydroxide layers. Formation of LDH with the cations ratio,  $n = (1-x)/x = M^{2+}/M^{3+}$ , of 2 and 3 is the most favourable

[Duan and Evans, 2006]; nevertheless, the compositions with  $n$  from 1 to 5 are possible, which provides a wide range of the layer charge per formula unit [Rives, 2001; Duan and Evans, 2006]. This feature offers additional flexibility to intercalate various negatively charged species different in nature, size, and charge: from monoatomic anions to huge organic complexes. As a result, the basal spacing value ( $d$ ), which is the distance between the mixed metal hydroxide layers (a sum of the layer thickness and the interlayer gallery height) can vary from about 7.5 to ~34 Å [Duan and Evans, 2006; Carrasco et al., 2018]. LDH are capable of non-destructive change of the chemical composition via anion exchange. Such properties of LDH find applications in corrosion protection, water purification, gas sensing, drug delivery, and many others [Neves et al., 2019; Zubair et al., 2017; Polese et al., 2015; Mishra et al., 2018]. Besides, these materials can be exfoliated into nanosheets and used for the design of complex artificial structures and nanocomposites

\* Corresponding author.

E-mail address: [salak@ua.pt](mailto:salak@ua.pt) (A.N. Salak).

<https://doi.org/10.1016/j.clay.2023.106843>

Received 15 August 2022; Received in revised form 10 January 2023; Accepted 23 January 2023

0169-1317/© 2023 The Authors. Published by Elsevier B.V. This is an open access article under the CC BY-NC-ND license (<http://creativecommons.org/licenses/by-nc-nd/4.0/>).

[Taviot-Guého et al., 2017].

Magnetic cations in positions of  $M^{2+}$  or/and  $M^{3+}$  provide LDH with new functionalities and make them of additional interest from both the application and fundamental points of view. The onset of spontaneous magnetisation and a peak of the magnetic susceptibility, in the LDH with  $M^{2+} = \text{Co}$  or  $\text{Ni}$  were observed below about 15 K [Intissar et al., 2002; Coronado et al., 2008; Coronado et al., 2010; Giovannelli et al., 2012; Vieira et al., 2017]. At the same time, magnetic LDH demonstrate glassy magnetic properties at low temperatures [Coronado et al., 2008; Carrasco et al., 2018]. The nature of the low-temperature magnetic phenomena in those LDH is still not completely clear. In particular, the questions arise if there is true long-range ferromagnetic ordering, and how magnetic ordering and glass behaviour coexist. A comparative study of low-temperature heat capacity and magnetisation would contribute to the clarification of the issue. The heat capacity behaviour of  $\text{Ni-Al}$  and  $\text{Ni-Fe}$  layered double hydroxides has been reported [Coronado et al., 2008]. No  $\lambda$ -peak nor Schottky-like anomaly has been detected. The anomaly of the temperature-dependent heat capacity was observed at higher temperatures as compared to the temperature of the magnetic susceptibility peak. It was concluded that no long-range magnetic ordering occurs in these LDH and they are rather spin glasses [Coronado et al., 2008]. To the best of our knowledge, no low-temperature heat capacity study of  $\text{Co}^{2+}$ -containing LDH has been carried out so far.

The magnetic properties of LDH are determined by a combination of in-plane superexchange interaction via oxygen bonds and the interlayer dipolar interaction [Carrasco et al., 2018]. The influence of dipolar interactions on the magnetic properties of LDH containing only one magnetic metal is very small. Thus, in  $\text{Co-Al}$  LDH, the interlayer interaction is about two orders of magnitude weaker than the superexchange one [Carrasco et al., 2018].

The magnetic properties of  $\text{Co}_n^2+\text{Al}^{3+}$  LDH are affected by their structural features. The continuous cobalt-cobalt magnetic exchange bonds are partly disrupted by aluminium cations. In the 2D hexagonal lattice with a statistical distribution of cations, the magnetic site's percolation limit (0.5) is exceeded for the LDH with  $n \geq 2$ . However, the presence of clusters with translational order of  $\text{Co}$  and  $\text{Al}$  may increase the percolation rate. The deviation from the ideal statistical cations distribution has been detected in our experiment with the magnetic-field assisted deposition of the  $\text{Co}_2\text{Al}$  LDH films [Vieira et al., 2021]. We have shown that the LDH nanoflakes demonstrate uniaxial magnetic anisotropy, which is only possible if a non-statistical distribution of  $\text{Co}$  and  $\text{Al}$  takes place in the hydroxide layers of this LDH. Another structural feature arises from the considerable difference between the ionic radii of  $\text{Co}^{2+}$  (0.75 Å) and  $\text{Al}^{3+}$  (0.57 Å), which leads to a strong distortion of the cobalt hydroxyl framework depending on the pattern of the  $\text{Co-Al}$  nearest neighbours. As a result, the cobalt energy levels, orbitals, and g-factors demonstrate large varieties [Vieira et al., 2021; Babkin et al., 2019]. The cobalt-cobalt nearest-neighbour superexchange interaction becomes non-unique due to variation of the  $\text{Co-O-Co}$  angles and different orientation of orbitals. The aforementioned interrelations between crystal structure and magnetic properties forms prerequisites for a spin glass behaviour or at least for a long-range non-uniform magnetic order in  $\text{Co-Al}$  LDH.

In the present work, we systematically studied the heat capacity and the magnetic behaviour of cobalt-aluminium LDH ( $n = \text{Co/Al} = 2$  and  $3$ ) intercalated with different inorganic and organic anions  $A^y$  (hereafter,  $\text{Co}_n\text{Al-A}$  LDH), which provided a series of compositions with the  $d$  value in the range of 7.6–16.6 Å. The heat capacity was measured as a function of temperature and applied magnetic field and compared with the temperature- and the field-dependences of the magnetic susceptibility. Using the method of a Modified Crystal Field Theory (MCFT) [Lamonova et al., 2019] we have created a theoretical model, which simulates the general features of the observed heat capacity anomalies. We have demonstrated a two-dimensional character of the magnetic contribution to the heat capacity of the cobalt-containing LDH and an important role

of the exchange interactions caused by various cation coordinations of  $\text{Co}^{2+}$  in the  $\text{Co-Al}$  hydroxide layers. Our zero-field heat capacity data for all studied LDH show a Schottky-type anomaly, which, however, does not have a  $\lambda$ -peak shape, which indicates the absence of magnetic long-range order in studied  $\text{Co}$ -based LDH.

## 2. Experimental details

The parent  $\text{Co}_2\text{Al-NO}_3$  and  $\text{Co}_3\text{Al-NO}_3$  LDH were synthesized using the conventional co-precipitation method from nitrate salts of the respective metals. Proportions of the reagents were chosen to meet the desired molar cation ratios without any excess. The compositions with  $n = 2$  and  $3$  were synthesized at the same conditions. More details on the synthesis of the parent  $\text{Co}_n\text{Al-NO}_3$  compositions can be found in Ref. [Salak et al., 2019].

To obtain LDH with different distances between the mixed metal hydroxide layers (basal spacings,  $d$ ), the parent LDH compositions were intercalated with the following anion species: hydroxide, carbonate, chloride, vanadate, gluconate, and mercaptobenzothiazolate via the respective anion exchange reactions in the solution containing these species [Salak et al., 2013; Serdechnova et al., 2016]. The compositions mentioned hereafter as  $\text{Co}_n\text{Al-OH}$ ,  $\text{Co}_n\text{Al-CO}_3$ ,  $\text{Co}_n\text{Al-Cl}$ ,  $\text{Co}_n\text{Al-VO}_3$ ,  $\text{Co}_n\text{Al-GNT}$ , and  $\text{Co}_n\text{Al-MBT}$  were thereby prepared.

X-ray diffraction (XRD) study of the obtained LDH powders was performed using a Rigaku D/MAX-B diffractometer in  $\text{Cu K}\alpha$  radiation. XRD data were collected in a step mode (step  $0.02^\circ$ , 20 s per step) at room temperature. Lattice parameters (in a hexagonal setting) of the LDH compositions and their basal spacings were calculated from the  $2\theta$  positions of the diffraction reflections (00l) and (110) (see Table S1 in Supplementary Material).

For magnetic measurements, the LDH powders were compacted into discs of about 3 mm in diameter and about 0.3 mm thick. Static magnetic properties of these samples were studied using a SQUID magnetometer technique (Quantum Design MPMS3) between 2 and 300 K in the magnetic field of up to 50 kOe in both zero-field-cooled (ZFC) and field-cooled (FC) modes.

The temperature dependence of heat capacity  $C(T)$  was measured using the Quantum Design Physical Properties Measurement System (PPMS) over the range of 1.9–150 K in a magnetic field up to 50 kOe.

The energy levels of  $\text{Co}^{2+}$  ions ( $3d^7$ -configuration,  $^4F$  basic term, six Kramers doublets) under influence of the spin-orbit interaction for all possible octahedral distortions [Babkin et al., 2019] and directions of the magnetic field were calculated using the MCFT method [Lamonova et al., 2019]. The main parameter of MCFT is the effective nuclear charge  $Z_{\text{eff}}$  of the central ion, which depends on the strength of the crystal field.

## 3. Results and discussion

### 3.1. Low-temperature Schottky-like anomaly in the heat capacity of $\text{Co}_n\text{Al}$ LDH

The Schottky anomaly, namely a maximum in the temperature dependence of the heat capacity at low temperatures, is associated with a splitting of the energy levels of paramagnetic ions in the crystal field [Tari, 2003]. At near-zero temperatures, only the lowest energy level is occupied. When the temperature rises and approaches the energy difference between the split levels, the upper split-off level is populated, and a peak is observed in the temperature dependence of the heat capacity, which corresponds to a sharp change in entropy with a small change in temperature [Beznosov et al., 2011]. The Schottky-like anomalies as the evidence of discrete energy states were observed for different  $\text{Co}$ -containing oxides, for example,  $\text{LaCoO}_3$  and double perovskites  $\text{Sr}_{2-x}\text{La}_x\text{CoNbO}_6$  [He et al., 2009; Kumar et al., 2020]. It was shown that no  $\lambda$ -anomaly occurs in the case of the composition with  $x = 0$ , which contains only  $\text{Co}^{3+}$  ions [Kumar et al., 2020]. However, for

the cases  $x > 0$  Schottky-like anomaly arises at low temperature and develops to higher  $T$  as the concentration of  $\text{Co}^{2+}$  ions increases. It is interesting that for  $x < 0.4$  it has a bump-like shape whereas for  $x > 0.4$  it has a shape close to a  $\lambda$ -peak. In  $\text{SrLaCoNbO}_6$  (for  $x = 1$ ), when all Co ions are in the oxidation state 2+, it transforms into classical  $\lambda$ -peak at the temperature of the 3D magnetic ordering,  $T_N = 14.7$  K [Kumar et al., 2020].

We revealed that the LDH under study, which are all  $\text{Co}^{2+}$ -containing, demonstrate the Schottky-like anomaly. Their heat capacity measured as a function of temperature was found to exhibit a hump in the  $C(T)$  dependence below 10 K (Fig. 1). Since  $\text{Co}^{2+}$  is a  $3d^7$  Kramers ion, the observed feature can be identified as a magnetic Schottky-like anomaly caused by the splitting of the ground-state Kramers doublet in the internal exchange field.

The Schottky-like anomaly in the studied  $\text{Co}_n\text{Al}$  LDH is broadened, which indicates a certain range of the splitting energy distribution. The observed broadening is in accordance with the presence of various types of octahedral hydroxyl cage distortions, i.e., with some scatter of the exchange interaction magnitude. The anomaly is strongly dependent on the applied magnetic field, which confirms its magnetic nature (Fig. 1). The hump in the  $C(T)$  curve shifts towards higher temperatures and broadens with an increasing external magnetic field, which contributes

to the action of the internal molecular field. Another manifestation of the magnetic nature of the observed heat capacity anomaly was detected at the lowest temperature of our experiment  $T_{min} = 1.9$  K: an increase of the external magnetic field resulted in gradual suppression of  $C(T_{min})$  (insets in Fig. 1). This indicates that the number of low-energy levels decreases because the splitting of Kramers doublets as a whole increases under the action of a magnetic field.

Despite the obvious magnetic origin of Schottky-type anomalies in all the samples studied, these anomalies demonstrate no zero-field  $\lambda$ -peak shape characteristic for the occurrence of the conventional three-dimensional magnetic ordering. This observation rules out the possibility of a long-range magnetic ordering in the  $\text{Co}^{2+}$ -containing LDH.

Fig. 2 shows the temperature-dependent heat capacity of the  $\text{Co}_n\text{Al}$  LDH intercalated with different anions that resulted in a wide range of basal spacing values from  $d = 7.6$  Å ( $\text{Co}_2\text{Al-CO}_3$ ) to  $16.6$  Å ( $\text{Co}_2\text{Al-MBT}$ ). The low-temperature heat capacity data (below 10 K) are considered as a sum of two contributions:  $C(T) = \beta T^3 + C_{mag}(T)$ , where the first term is a low-temperature approximation for the lattice contribution, the second one is the magnetic contribution. No electronic contribution has to be considered in the studied magnetic insulator. The temperature dependences were presented as  $C/T^2$  versus  $T$  to highlight the magnetic

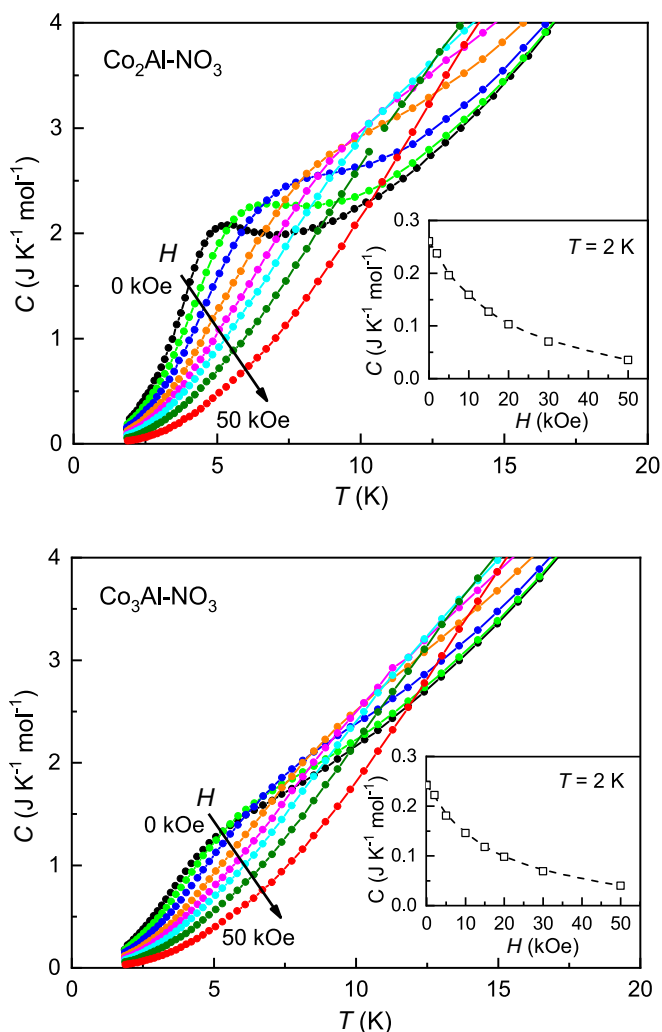


Fig. 1. Temperature-dependent heat capacity  $C(T, H)$  of  $\text{Co}_2\text{Al-NO}_3$  LDH (top panel) and  $\text{Co}_3\text{Al-NO}_3$  LDH (bottom panel) measured in an external magnetic field of 0, 2, 5, 10, 15, 20, 30, and 50 kOe. Insets: a characteristic decrease of the heat capacity with the increasing magnetic field at the lowest measured temperature,  $T = 2$  K.

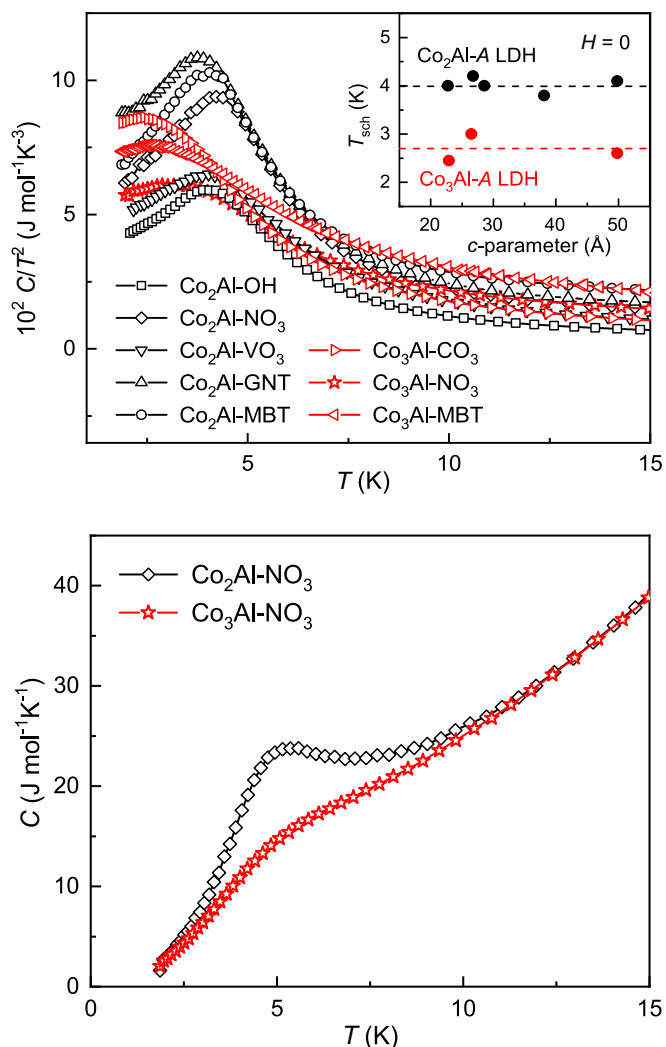


Fig. 2. Top panel: temperature-dependent heat capacity of  $\text{Co}_n\text{Al}$  LDH (intercalated with different anions  $A$ ) measured in a zero magnetic field and plotted as  $C/T^2$  versus  $T$ . The inset shows the temperature of the Schottky-like anomaly,  $T_{sch}$  (see definition in the text), as a function of the lattice parameter  $c = 3d$ . Bottom panel: the normalized  $C$  vs  $T$  plots for  $\text{Co}_2\text{Al-NO}_3$  and  $\text{Co}_3\text{Al-NO}_3$  LDH.

part of the heat capacity. It is evident from Fig. 2a that the Schottky-like anomaly is much more pronounced for the LDH with Co/Al ratio of 2 (in black) than for a ratio of 3 (in red). The difference in Schottky-like contribution to the low-temperature heat capacity for LDH with  $n = 2$  and 3 is clearly seen in Fig. 2b.

The Schottky-like contribution to the heat capacity is dependent on the energy gap between split levels ( $\Delta$ ) and for the simplest two-level system can be represented as [Tari, 2003]:

$$C_{Sch} = R \cdot \left(\frac{\Delta}{T}\right)^2 \cdot \frac{e^{\frac{\Delta}{T}}}{(1 + e^{\frac{\Delta}{T}})^2},$$

where  $R = 8.314 \text{ J/mol}\cdot\text{K}$  is the universal gas constant. In the case of a set of gaps, the width of the Schottky maximum depends on the distribution of the gap's energies. The difference in the low-temperature heat capacity for the compositions with Co/Al ratios of 2 and 3 (Fig. 2b) is associated with the widening of energy spectra distribution for  $\text{Co}^{2+}$  ion in LDH with  $n = 3$  as compared to that with  $n = 2$  due to different set of distortions of hydroxyl octahedra surrounding a cobalt ion.

One can see from the inset in Fig. 2a that the temperature of the Schottky-like anomaly,  $T_{Sch}$ , defined as a position of the  $C/T^2$  peak in a zero external field, is near the same (about 4 K) for all the LDH with  $n = 2$ . For the LDH with  $n = 3$ ,  $T_{Sch}$ , is also rather independent of the  $d$ -value but smaller, namely  $\sim 2.7 \text{ K}$ .

The impact of the external magnetic field on the Schottky-like anomaly is clearly seen in Fig. 3, which represents the plots  $C/T^2$  versus  $T$  measured in different magnetic fields. The field dependences of the Schottky-like anomaly temperature,  $T_{Sch}(H)$ , of all the studied LDH compositions are very similar regardless of the intercalated anion

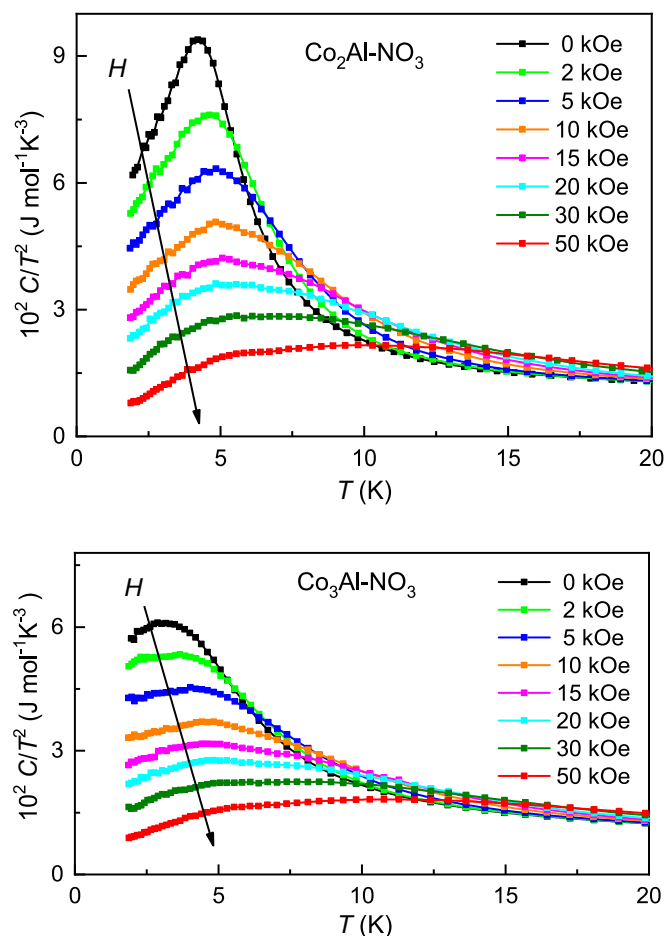


Fig. 3. The variation of the Schottky-like anomaly with magnetic field for  $\text{Co}_2\text{Al-NO}_3$  LDH (top panel) and  $\text{Co}_3\text{Al-NO}_3$  LDH (bottom panel).

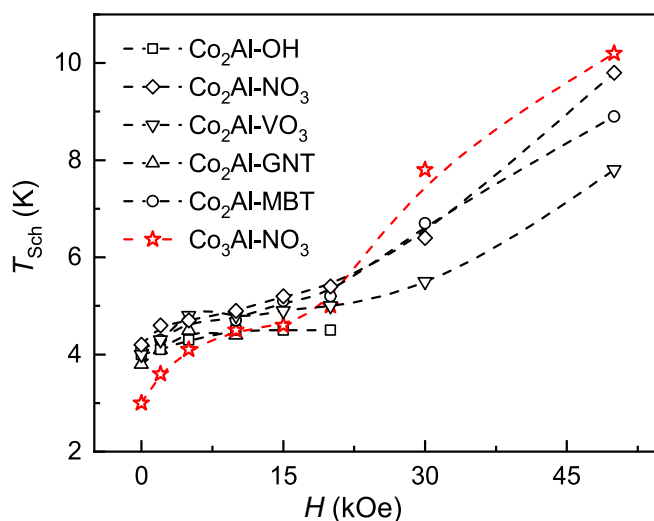


Fig. 4. The Schottky-like anomaly temperature,  $T_{Sch}$ , of  $\text{Co}_n\text{Al}$  LDH as a function of the applied magnetic field for different intercalated anions. Dashed lines are guides to the eye.

(Fig. 4). The  $T_{Sch}$  value gradually increases with field. Above about 20 kOe, the increment linearly rises. It means that the magnetic field value at which this occurs evidently exceeds the value of the internal molecular field.

### 3.2. Low-temperature magnetic ordering of $\text{Co}_n\text{Al}$ LDH: Effects of the cations ratio and the basal spacing

A systematic study of the magnetic properties of  $\text{Co}_n\text{Al}$  LDH ( $n = 2$ ) intercalated with different organic anions has recently been reported [Carrasco et al., 2018]. The compositions with the basal spacing  $d$  of 7.59, 14.96, 21.76, 26.68, and 33.84 Å were prepared and thoroughly characterized. In the present work, we studied  $\text{Co}_n\text{Al}$  ( $n = 2$  and 3) LDH with the basal spacing ranging from 7.59 to 16.61 Å and smaller  $d$ -value increments (Table S1 of Supplementary Material).

In each LDH studied, a peak of the magnetic susceptibility has been detected in the same temperature range below 10 K, where a Schottky-like anomaly was observed. Zero-field cooled magnetisation curves,  $M(T)$ , appeared to be very similar to the temperature-dependent heat capacity curves,  $C/T^2$  vs.  $T$ , in shape, power, and temperature position of the maxima (Fig. 5). For instance, the  $T_{Sch}$  values determined in this

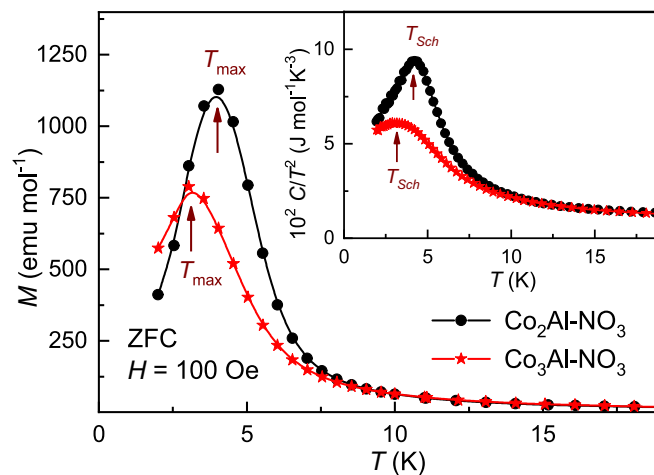


Fig. 5. The temperature-dependent magnetic moment,  $M$ , of  $\text{Co}_2\text{Al-NO}_3$  and  $\text{Co}_3\text{Al-NO}_3$  LDH measured in a ZFC mode. Inset: the  $C/T^2$  vs  $T$  plots of the same LDH measured in a zero magnetic field.

work are 3.0 K for  $\text{Co}_3\text{Al-NO}_3$  and 4.0 K for  $\text{Co}_2\text{Al-NO}_3$ , while the temperatures of the maxima in the ZFC  $M(T)$  dependences,  $T_{\text{max}}$ , are 3.2 and 4.0 K, respectively, (Fig. 5). Both the heat capacity anomalies and the magnetic peaks are much less pronounced for the  $\text{Co}_3\text{Al}$  LDH than for that with  $n = 2$  (Fig. 5). It is evident of the close interconnection of the magnetism of LDH studied and the Schottky-like anomaly observed in these compositions.

We previously reported that the low-temperature ZFC and FC static magnetisation curves of  $\text{Co}_n\text{Al-NO}_3$  LDH ( $n = 2,3$ ) diverge with decreasing temperature and the splitting begins slightly above  $T_{\text{max}}$  [Vieira et al., 2017]. In this work, the measurements performed on the  $\text{Co}_n\text{Al}$  LDH intercalated with other anions revealed that such a divergence, associated with the highly anisotropic and/or glassy magnetic state, is a common feature of the  $\text{Co}^{2+}$ -containing layered hydroxides. Fig. 6a demonstrates this feature for the particular case of  $\text{Co}_2\text{Al-GNT}$  LDH.

Besides, all the LDH studied demonstrate magnetic hysteresis loops at low temperatures (Figs. 6b and 7), which are together with a form of the temperature-dependent ZFC and FC static magnetisation curves, are evident of the ferromagnetic ordering. The values of the coercive field,  $H_c \sim 95\text{--}120$  Oe at 1.8 K for  $\text{Co}_2\text{Al}$  LDH, are relatively high in comparison with the internal exchange magnetic field which was estimated to be of about 14 kOe at  $T = 0$  K (Section 3.3). We have found no correlation between the coercive field and basal spacing value for the

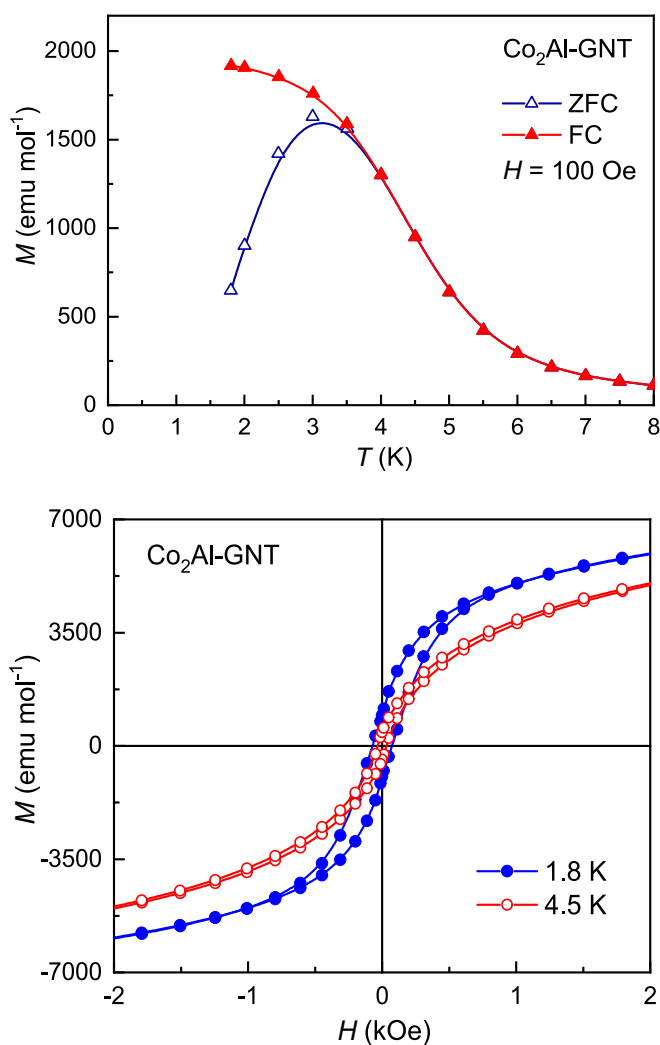


Fig. 6. The static magnetic moment of  $\text{Co}_2\text{Al-GNT}$  LDH measured in ZFC and FC modes (top panel). Low-temperature magnetic hysteresis loops of  $\text{Co}_2\text{Al-GNT}$  LDH (bottom panel).

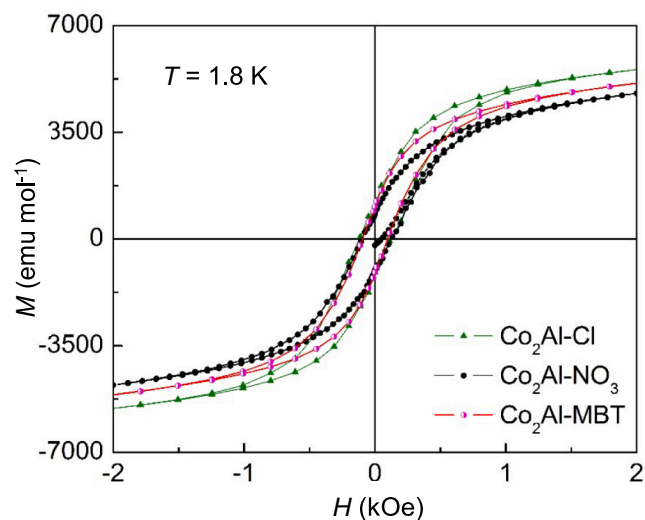


Fig. 7. Low-temperature magnetic hysteresis loops of some  $\text{Co}_2\text{Al}$  LDH measured at 1.8 K.

studied LDH, which is in complete agreement with the results reported in Ref. [Carrasco et al., 2018].

The temperature of the magnetization onset,  $T_C$ , was obtained as the intersection of the linear ranges of the ZFC  $M(T)$  curve above and below the temperature of a sharp increase in magnetisation. The  $T_C$  value for the LDH with  $n = 2$  appeared to be dependent on the interlayer distance for the low basal spacing only (Fig. 8). It decreases almost linearly with an increase in the basal spacing up to about 10 Å and demonstrates no correlation with a further increase in  $d$ . Since the LDH with  $n = 3$  exhibited less pronounced magnetisation peaks as compared to those observed in LDH with  $n = 2$ , the error in the determination of their  $T_C$  was larger. Nevertheless, the overall behaviour of  $T_C$  versus  $d$  for the cases of  $n = 2$  and 3 is very similar. The results of our study of the magnetic properties of  $\text{Co}_n\text{Al}$  LDH in connection to their basal spacing (at least, for  $d$ -values above  $\sim 10$  Å) agree well with the conclusion of Ref. [Carrasco et al., 2018] that an increase in the interlayer distance weakly affects the dipolar interaction.

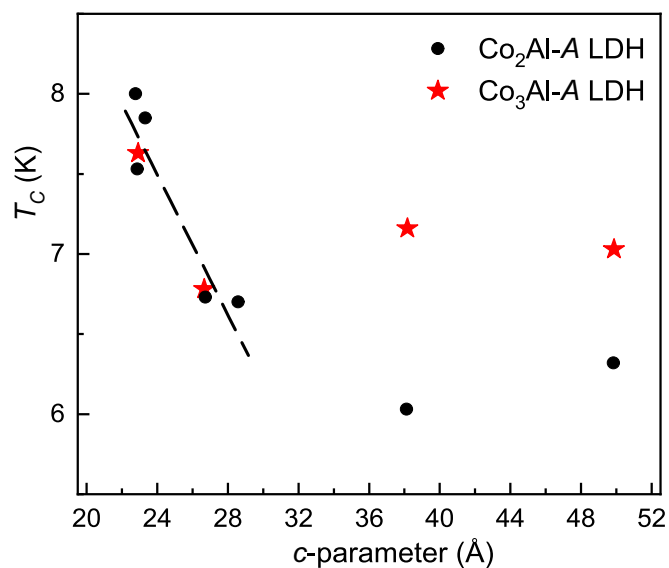


Fig. 8. The temperature of magnetization onset,  $T_C$ , versus the lattice  $c$ -parameter ( $c = 3d$ , where  $d$  is the basal spacing value) for  $\text{Co}_2\text{Al}$  and  $\text{Co}_3\text{Al}$  LDH intercalated with different anions  $A$ . The values of  $c$ -parameters of the  $\text{Co}_n\text{Al-A}$  LDH are listed in Table S1 of Supplementary Material.

The obtained data indicate that the low-temperature magnetic behaviour of  $\text{Co}_n\text{Al}$  LDH, similar to that of their heat capacity, depends mainly on the cobalt content in the mixed metal hydroxide layers.

### 3.3. Theoretical modelling of the magnetic heat capacity

Magnetic properties of the  $\text{Co}_n^{2+}\text{Al}^{3+}$  LDH in the experimental range are affected by four of the six lowest Kramers doublets of the  $\text{Co}^{2+}$  ion in the octahedral hydroxyl environment ( $3d^7$ -configuration,  $^4\text{F}$  base term) with energies  $kT \sim < 300$  K [Babkin et al., 2012]. Internal exchange magnetic fields split the ground state Kramers doublet. The gap value is determined by the Co—Co nearest-neighbour exchange interactions. We have recently considered thirteen possible types of nearest coordination of cobalt cations in  $\text{Co}_n\text{Al}$  LDH (Fig. S1 of *Supplementary Material*) and calculated their statistical weights for cases of  $n = 2, 3$ , and 4 [Babkin et al., 2019; Vieira et al., 2021]. A simple structural model of the corresponding 13 hydroxyl octahedra distortions, which takes into consideration the radii of the involved ions, was developed and used in further calculations. One can see from the results (Table S2 of *Supplementary Material*) that for each type of coordination, the central cobalt ion has a particular energy spectrum and orbital orientation specific to its ground state.

According to the Goodenough-Kanamori rules the value of the nearest-neighbour exchange interactions depends on the angle of the metal-ligand-metal bonds and the orbital states for both metals. One can show that thirteen types of cobalt orbital states together with specific distortions of its hydroxyl cages create forty-five Co—Co nearest-neighbour magnetic exchange pathways. The multiplicity of exchange interactions forms some gap energy distributions. However, the number of exchange pathways depends on the statistical distribution of Co positions. For instance, in the case of ideal translation symmetry of Co—Al positions in the LDH with  $n = 2$ , in which every aluminium cation has six cobalt cations as nearest neighbours and every cobalt cation is surrounded by three  $\text{Co}^{2+}$  and three  $\text{Al}^{3+}$  (named as the  $h$ -type, see *Supplementary Material*), the only one type of exchange interaction exists. In such a case of the so-called 2:1 long-range order, the Schottky-like anomaly should be the sharpest as it is induced by only one gap. In the opposite case of a fully random Co—Al distribution, one should expect the smoothing of a Schottky-like maximum resulting from a wide energy gap distribution.

Let us apply the above speculations to the low-temperature heat capacity behaviour observed in cobalt-aluminium LDH. From a qualitative point of view, the narrower Schottky-like peak of the  $\text{Co}_2\text{Al-NO}_3$  LDH as compared to that of the  $\text{Co}_3\text{Al-NO}_3$  LDH (see Fig. 3b) evidences a presence of a Co—Al translational order in the former and a rather random cation distribution in the latter. In our previous study, we found no superlattice diffraction reflections, which are characteristic of a 2:1 long-range cation order in  $\text{Co}_2\text{Al-NO}_3$  [Vieira et al., 2021]. At the same time, we detected magnetic anisotropy of the flake-like nanocrystallites of this LDH, which makes them oriented in the magnetic field to be perpendicular to the flake plane, and demonstrated numerically that such anisotropy is only possible if the distribution of cobalt and aluminium is not statistical. It followed from our calculations that in  $\text{Co}_2\text{Al-NO}_3$  and other LDH prepared via anion exchange using this cobalt-aluminium nitrate layered hydroxide as a parent composition, the probability of the  $h$ -type of the cobalt cation coordination (see Fig. S1 of *Supplementary Material*) prevails over its statistical weight.

Here we applied the aforementioned structural model of 13 hydroxyl octahedra distortions to simulate the temperature and field dependences of the magnetic part of specific heat of the  $\text{Co}_2\text{Al-NO}_3$  LDH. The internal magnetic field value as well as its temperature behaviour in a mean-field approximation was extracted from the temperature-dependent magnetisation of this composition measured on compacted powder samples upon the FC process with a field of 100 Oe [Vieira et al., 2017]. It was assumed that: a) the *uniform* internal magnetic field acts on the set of statistically distributed cobalt positions and it has to reproduce the value

and temperature dependence of the magnetisation; b) the existing magnetic anisotropy is accounted for by a direction of the internal magnetic field which is perpendicular to octahedral layer, i.e. along the  $z$ -axis; c) due to the powder sample and anisotropy the measured magnetisation value is lower than the true one by a factor of three. The obtained temperature dependence of the internal magnetic field in the  $\text{Co}_2\text{Al-NO}_3$  LDH is shown in Fig. 9.

We apply the extracted  $H_{\text{int}}(T)$  behaviour to calculate the temperature- and the field-dependent magnetic contribution to the heat capacity,  $C_m(H, T)$ , in the  $\text{Co}_2\text{Al-NO}_3$  LDH. (For details of the calculation see *Supplementary Material*). The obtained  $C_m$  vs.  $T$  curves at different values of the external field are shown in Fig. 10.

Even in our oversimplified model for the internal field, it was possible to reproduce the main feature of the temperature and the field dependences of the measured heat capacity. However, to match the theoretical results with the experimental value of  $T_{Sh} = 4$  K at zero external field, we had to use a modified distribution of Co positions, in which the weight of the  $h$ -type of the cobalt cation coordination is increased by a factor of three as compared to that in the ideal statistical distribution (c.f.:  $w_H = 0.075$  versus 0.025, *Supplementary Material*). Notice, that the artificially increased weight of the  $h$ -type coordination nevertheless remains relatively small.

It should be stressed here that the above analysis and conclusions done based on the assumption of the non-statistical cation distribution and regions with a 2:1 Co—Al ordering in  $\text{Co}_2\text{Al-NO}_3$  are entirely applicable for other  $\text{Co}_2\text{Al}$  LDH under study. These LDH were prepared from the parent  $\text{Co}_2\text{Al-NO}_3$  using anion substitution reactions, at which the cation composition and structure of the hydroxide layers remain unchanged. It is important to notice that full translational order in a  $\text{Co}_2\text{Al}$  LDH can be constructed entirely from the  $h$ -coordination; therefore, the presence of regions with a 2:1 Co—Al ordering in such LDH is thermodynamically favourable as it decreases the system entropy. On the other part, the translational order in the  $\text{Co}_3\text{Al}$  LDH cannot be built using only the  $h$ -type coordination and LDH is in the case of the fully statistical Co—Al distribution its statistical weight is rather small ( $w_H = 0.013$  [Babkin et al., 2019]). Therefore, a lack of sufficient contribution of  $h$ -coordination into heat capacity leads to smearing and widening of the Schottky-like maximum in the  $\text{Co}_3\text{Al}$  LDH as compared to that in the  $\text{Co}_2\text{Al}$  LDH (Fig. 2).

In the magnetic field, the ground-state Kramers doublet energy gap distribution shifts towards a higher energy range and widens. The appearance of the field-induced high-energy gaps expectedly leads to the broadening of the Schottky-like maximum, which occurs even under the condition of a single high-energy level. As a result of the spreading of the energy gap distribution, the maximum lowers and broadens with increasing magnetic field although remains visible in the  $C(H, T)/T^2$

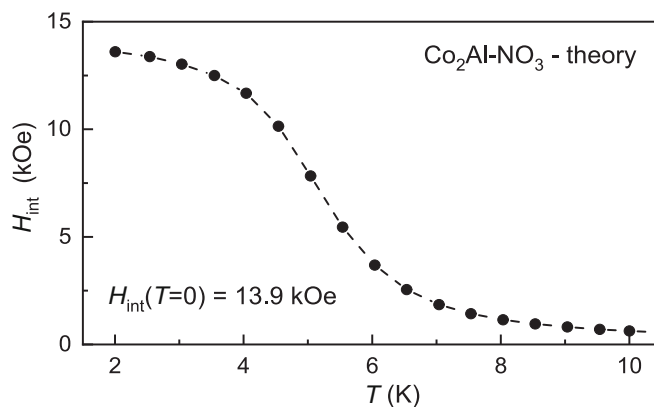
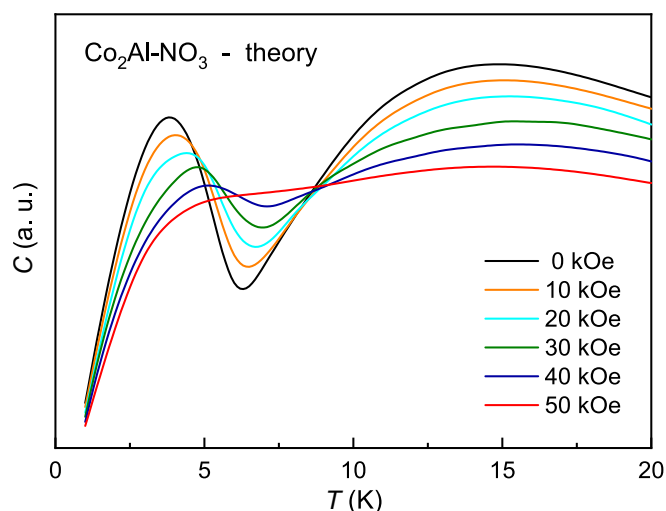


Fig. 9. The temperature-dependent internal magnetic field,  $H_{\text{int}}(T)$ , in the  $\text{Co}_2\text{Al-NO}_3$  LDH calculated under the assumption that  $H_{\text{int}}$  is uniform and directed perpendicular to the octahedral layer (along  $z$ -axis).



**Fig. 10.** The temperature-dependent magnetic contribution to the heat capacity of  $\text{Co}_2\text{Al-NO}_3$  LDH calculated for the external magnetic fields in the range of 0–50 kOe.

representation even at the highest magnetic field of 50 kOe in our experiment (Fig. 3).

There are two distinctive features of the magnetic field-induced behaviour of heat capacity of the  $\text{Co}^{2+}$ -containing LDH, namely (i) the nonlinear dependence of the heat capacity  $C(T_{min})$  on magnetic field at  $T = 2$  K shown in insets of Fig. 1 and (ii) the nonlinear dependence of the Schottky-like anomaly temperature  $T_{Sch}$  on the magnetic field below 20 kOe (Fig. 4). Note that in the case of pure ferromagnetic ordering with a single unique exchange, both these parameters should demonstrate a linear behaviour. Thus, the observed nonlinearity indicates the presence of the regions with non-uniform magnetic order in these LDH, which is caused by a variety of available exchange pathways. The magnetic pattern of the cobalt-containing LDH can be represented as the regions with a 2:1 Co–Al ordering, which are embedded into the double-metal hydroxide matrix that is a mix of the remaining 12 coordinations (with a particular Co–Co exchange interaction each). These regions exhibit a uniform ferromagnetic order, while the matrix is magnetically non-uniform. Such a magnetic structure is expected to result in a cluster spin-glass behaviour. Furthermore, in this case, the exchange interactions are involved in the formation of the coercivity mechanism. Indeed, the relatively large difference between the coercive field value ( $H_c \sim 10^2$  Oe) and the average internal field value ( $H_{int} \sim 10^4$  Oe) instead of typical for  $\text{Co}^{2+}$  Kramers ions relation  $H_c \sim H_a$  where  $H_a$  is anisotropy and  $H_a \sim 10^{-4} H_{int}$  is evidence of a such effect.

When the external magnetic field sufficiently exceeds the averaged internal field, the  $T_{Sch}(H)$  dependence becomes linear since the field suppresses the non-uniform magnetic order and a collinear ferromagnetic one occurs. This case is realised in the samples under study for the external field above  $H_{int} = 13.9$  kOe (Fig. 4).

No detected correlation between the interlayer distance and the Schottky-like anomaly temperature (see inset in Fig. 2) points out that only intralayer exchange interactions contribute to the magnetic part of the heat capacity of cobalt-aluminium LDH.

#### 4. Conclusions

The low-temperature magnetic behaviour of  $\text{Co}_n^2+\text{Al}^{3+}$  LDH ( $n = 2, 3$ ) is determined by the splitting and population of the lowest doublets of  $\text{Co}^{2+}$ , which in their turn are dependent on the thirteen possible distortions of the surrounding hydroxyl octahedra. The low-temperature heat capacity of these LDH demonstrates the Schottky-like peak attributed to the energy gaps opened because of the splitting of the ground state Kramers doublet in the internal exchange field. In all studied LDH

samples, the Schottky-like anomaly has no  $\lambda$ -peak shape that excludes the existence of the long-range magnetic order in these compounds. The external magnetic field shifts the peak towards higher temperatures with simultaneous smoothing and broadening indicating the magnetic origin of the effect. The anomalies in the temperature dependence of the heat capacity and the magnetisation are more pronounced for the LDH with  $n = 2$  than for those with  $n = 3$ . The theoretical calculations suggest that it may result from an excess of cobalt coordinations with a 2:1 Co–Al ordering (e.g. short-range clusters) over the statistical distribution in the  $\text{Co}_2\text{Al}$  compositions, whereas cation distribution in the  $\text{Co}_3\text{Al}$  LDH is random. The Schottky-like maximum temperature is different for the  $\text{Co}_n\text{Al}$  LDH with  $n = 2$  and  $n = 3$  and independent of the interlayer distance, which is a manifestation of the entirely intralayer internal exchange contribution to their heat capacities. A comparison of the measured coercive field and the calculated internal field indicates that the exchange interactions caused by various coordinations of cobalt contribute to the mechanism of the coercive field formation. The observed field-induced features in the heat capacity provide evidence of the presence of regions with a non-uniform magnetic order in these LDH, in which are incorporated ferromagnetic clusters with 2:1 Co–Al structural order. These observations, as well as the absence of the long-range magnetic order, allow us to suggest the existence of the cluster spin glass magnetic ground state in  $\text{Co}_n^2+\text{Al}^{3+}$  LDH ( $n = 2, 3$ ) under study.

#### Declaration of Competing Interest

The authors declare that they have no known competing financial interests or personal relationships that could have appeared to influence the work reported in this paper.

#### Data availability

Data will be made available on request.

#### Acknowledgements

This work was supported by the EU H2020 project European Microkelvin Platform (EMP), grant agreement No. 824109. Yu. G. Pashkevich acknowledges the financial support of the Swiss National Science Foundation through the individual grant IZSEZO\_212006 of the «Scholars at Risk» Program. D.E.L. Vieira acknowledges the financial support of FCT-Portugal through the individual PhD grant PD/BD/143033/2018. A.N. Salak and C.S. Neves acknowledge the financial support of national funds (OE) through FCT-Portugal in the scope of the framework contract foreseen in the numbers 4, 5 and 6 of the article 23, of the Decree-Law 57/2016, of August 29, changed by Law 57/2017, of July 19. The research done in the University of Aveiro was supported by the project CICECO-Aveiro Institute of Materials, UIDB/50011/2020, UIDP/50011/2020 & LA/P/0006/2020, financed by national funds through the FCT/MEC (PIDDAC). The research at P.J. Šafárik University was supported by the Slovak Research and Development Agency under grant No. APVV-18-0197 and by the Scientific Grant Agency of the Ministry of Education, Science, Research and Sport of the Slovak Republic under grant Nos. 1/0426/19 and 1/0512/23.

#### Appendix A. Supplementary data

Supplementary data to this article can be found online at <https://doi.org/10.1016/j.clay.2023.106843>.

#### References

- Babkin, R.Y., Lamonova, K.V., Orel, S.M., Pashkevich, Y.G., Meshcheryakov, V.F., 2012. Determination of the effective nuclear charge from EPR data using a modified crystal-field theory. *Opt. Spectrosc.* 112, 438–442.

- Babkin, R.Yu., Pashkevich, Yu.G., Fedorchenko, A.V., Fertman, E.L., Desnenko, V.A., Prokhvatilov, A.I., Galtsov, N.N., Vieira, D.E.L., Salak, A.N., 2019. Impact of temperature dependent octahedra distortions on magnetic properties of Co-containing double layered hydroxides. *J. Magn. Magn. Mater.* 473, 501–504.
- Bezanosov, A., Fertman, E., Desnenko, V., Kajnakova, M., Feher, A., 2011. The Nd-Mn exchange interaction, low temperature specific heat and magnetism of  $\text{Nd}_{2/3}\text{Ca}_{1/3}\text{MnO}_3$ . *J. Magn. Magn. Mater.* 323, 2380–2385.
- Carrasco, J.A., Cardona-Serra, S., Clemente-Juan, J.M., Gaita-Ariño, A., Abellán, G., Coronado, E., 2018. Deciphering the role of dipolar interactions in magnetic layered double hydroxides. *Inorg. Chem.* 57, 2013–2022.
- Coronado, E., Galan-Mascaros, J.R., Martí-Gastaldo, C., Ribera, A., Palacios, E., Castro, M., Burriel, R., 2008. Spontaneous magnetization in Ni-Al and Ni-Fe layered double hydroxides. *Inorg. Chem.* 47, 9103–9110.
- Coronado, E., Martí-Gastaldo, C., Navarro-Moratalla, E., Ribera, A., 2010. Intercalation of  $[\text{M}(\text{ox})_3]^{3-}$  (M=Cr, Rh) complexes into  $\text{Ni}^{\text{II}}\text{Fe}^{\text{III}}\text{-LDH}$ . *Appl. Clay Sci.* 48, 228–234.
- Duan, X., Evans, D.G., 2006. Layered double hydroxides Structure & Bonding, 119. Springer-Verlag Berlin Heidelberg, pp. 121–159.
- Giovannelli, F., Zaghrioui, M., Autret-Lambert, C., Delorme, F., Seron, A., Chartier, T., Pignon, B., 2012. Magnetic properties of  $\text{Ni}(\text{II})\text{-Mn}(\text{III})\text{-LDH}$ . *Mater. Chem. Phys.* 137, 55–60.
- He, C., Zheng, H., Mitchell, J.F., Foo, M.L., Cava, R.J., Leighton, C., 2009. Low temperature Schottky anomalies in the specific heat of  $\text{LaCoO}_3$ : Defect-stabilized finite spin states. *Appl. Phys. Lett.* 94, 102514.
- Intissar, M., Segni, R., Payen, C., Besse, J.P., Leroux, F., 2002. Trivalent cation substitution effect into layered double hydroxides  $\text{Co}_2\text{Fe}_y\text{Al}_{1-y}(\text{OH})_6\text{Cl } n\text{H}_2\text{O}$ : study of the local order. Ionic conductivity and magnetic properties. *J. Solid State Chem.* 167, 508–516.
- Kumar, A., Schwarz, B., Ehrenberg, H., Dhaka, R.S., 2020. Evidence of discrete energy states and cluster-glass behavior in  $\text{Sr}_{2-x}\text{La}_x\text{CoNbO}_6$ . *Phys. Rev. B* 102, 184414.
- Lamonova, K.V., Orel, S.M., Pashkevich, Yu.G., 2019. Modified Crystal Field Theory and its Applications. Akadempriodyka, Kyiv, 226 pp.
- Mishra, G., Dash, B., Pandey, S., 2018. Layered double hydroxides: a brief review from fundamentals to application as evolving biomaterials. *Appl. Clay Sci.* 153, 172–186.
- Neves, C.S., Bastos, A.C., Salak, A.N., Starykevich, M., Rocha, D., Zheludkevich, M.L., Cunha, A., Almeida, A., Tedim, J., Ferreira, M.G.S., 2019. Layered double hydroxide clusters as precursors of novel multifunctional layers: a bottom-up approach. *Coatings* 9, 00328.
- Polese, D., Mattocchia, A., Giorgi, F., Pazzini, L., Ferrone, A., Di Giamberardino, L., Maiolo, L., Pecora, A., Convertino, A., Fortunato, G., Medaglia, P.G., 2015. Layered double hydroxides intercalated with chlorine used as low temperature gas sensors. *Procedia Eng.* 120, 1175–1178.
- Rives, V., 2001. Double Hydroxides: Present and Future. Nova Science Publishers Inc., New York, USA, 439 pp.
- Salak, A.N., Tedim, J., Kuznetsova, A.I., Vieira, L.G., Ribeiro, J.L., Zheludkevich, M.L., Ferreira, M.G.S., 2013. Thermal behavior of layered double hydroxide Zn-Al-pyrovandate: composition, structure transformations, and recovering ability. *J. Phys. Chem. C* 117, 4152–4157.
- Salak, A.N., Vieira, D.E.L., Lukienko, I.M., Shapovalov, Yu.O., Fedorchenko, A.V., Fertman, E.L., Pashkevich, Yu.G., Babkin, R.Yu., Shilin, A.D., Rubanik, V.V., Ferreira, M.G.S., Vieira, J.M., 2019. High-power ultrasonic synthesis and magnetic-field-assisted arrangement of nanosized crystallites of cobalt-containing layered double hydroxides. *ChemEngineering* 3, 62.
- Serdechnova, M., Salak, A.N., Barbosa, F.S., Vieira, D.E.L., Tedim, J., Zheludkevich, M.L., Ferreira, M.G.S., 2016. Interlayer intercalation and arrangement of 2-mercaptobenzothiazolate and 1, 2, 3-benzotriazololate anions in layered double hydroxides: in situ X-ray diffraction study. *J. Solid State Chem.* 233, 158–165.
- Tari, A., 2003. The Specific Heat of Matter at Low Temperatures. Imperial College Press, London, 250 pp.
- Taviot-Guého, C., Prévot, V., Forano, C., Renaudin, G., Mousty, C., Leroux, F., 2017. Tailoring hybrid layered double hydroxides for the development of innovative applications. *Adv. Funct. Mater.* 1703868.
- Vieira, D.E.L., Salak, A.N., Fedorchenko, A.V., Pashkevich, Yu.G., Fertman, E.L., Desnenko, V.A., Babkin, R.Yu., Čizmar, E., Feher, A., Lopes, A.B., Ferreira, M.G.S., 2017. Magnetic phenomena in Co-containing layered double hydroxides. *Low Temp. Phys* 43, 977–981.
- Vieira, D.E.L., Cardoso, J.P.V., Fedorchenko, A.V., Fertman, E.L., Čizmar, E., Feher, A., Babkin, R.Yu., Pashkevich, Yu.G., Brett, C.M.A., Vieira, J.M., Salak, A.N., 2021. Magnetic-field-assisted deposition of self-assembling crystallite layers of  $\text{Co}^{2+}$ -containing layered double hydroxides. *Chem. Commun.* 57, 6899–6902.
- Zubair, M., Daud, M., McKay, G., Shehzad, F., Al-Harhi, M.A., 2017. Recent progress in layered double hydroxides (LDH)-containing hybrids as adsorbents for water remediation. *Appl. Clay Sci.* 143, 279–292.